Journal of ELECTRONIC MATERIALS, Vol. 49, No. 11, 2020
https://doi.org/10.1007/s11664-020-08434-x

Fabrication of Bacterial Cellulose-Based ATO-PPy Nanocomposites as Flexible Conductive Materials

JIANBIN YE,[1] LINXUAN GUO,[2] YINGJIE FENG,[3] FUYAN SUN,[1] TINGTING ZHANG,[3] ZONGCAN YANG,[3] GUOPENG SHEN,[2] and ZHAN ZHANG[3,4]

1.—School of Food and Biological Engineering, Zhengzhou University of Light Industry, Zhengzhou 450002, People's Republic of China. 2.—School of Chemical Engineering and Energy, Zhengzhou University, Zhengzhou 450001, People's Republic of China. 3.—Technology Center, China Tobacco Henan Industrial Co., Ltd., Zhengzhou 450001, People's Republic of China. 4.—e-mail: zhangzhan2059729@126.com

An ideal flexible conductive material, bacterial cellulose-based antimony tin oxide-polypyrrole (BC-ATO-PPy), was fabricated in this study. The BC-ATO film was synthesized in situ along with the growth of the BC film, and then PPy was coated uniformly onto the as-prepared film. The structural characterization results showed that BC-ATO-PPy was successfully fabricated. The electrochemical properties of these as-synthesized composites (BC-ATO-PPy, BC-PPy, BC-ATO) were better than those of pure BC. A cyclic voltammetry (CV) test showed that the conductivities of BC-ATO, BC-PPy and BC-ATO-PPy were increased to 10.236 S/cm, 11.636 S/cm and 16.532 S/cm, respectively. The electrochemical impedance spectra (EIS) test showed that the resistance values of BC-ATO, BC-PPy and BC-ATO-PPy decreased to 83.6 Ω, 63.2 Ω and 32.4 Ω, respectively. Additionally, the specific capacitance also increased from 7.47 F/g for BC to 681.3 F/g for BC-ATO-PPy, 563.9 F/g for BC-ATO and 302.2 F/g for BC-PPy. The bending test showed that BC-ATO-PPy has stable CV curves and conductivity, suggesting that it is an excellent flexible conductive material. These results suggested that these as-synthesized nanomaterials, especially BC-ATO-PPy, are ideal flexible conductive materials.

Key words: Bacterial cellulose, flexible, antimony tin oxide (ATO), PPy, conductive

INTRODUCTION

Flexible and stretchable conductive materials have attracted great attention due to their wide applications in optoelectronic devices.[1,2] For example, lightweight flexible conductive materials have largely promoted the development of portable electronic devices, including wearable electronics, touch screens and liquid crystal displays.[3,4] The growing demand for these products has resulted in the intense consumption of nonrenewable natural resources. Thus, great efforts should be made to develop renewable, biodegradable and environmentally friendly flexible conductive materials.

Cellulose, a biodegradable polymer, has been widely used as a support to fabricate flexible conductive nanomaterials that have been applied onto flexible displays, flexible solar cells and portable supercapacitors.[5,6] Compared to plant and animal cellulose, bacterial cellulose (BC) has gained considerable attention not only because of its excellent physicochemical properties but also because it is a sustainable polymer material produced by several special bacteria. Bacteria, such as *Ace-*

(Received April 12, 2020; accepted August 20, 2020; published online September 9, 2020)

tobacter xylinum,[7] synthesize BC by using pure sugar as a substrate. This makes the production of BC low-cost and environmentally friendly. The sugar molecules are connected by the bacteria, which makes BC an ultrafine nano-network structure with pores ranging from nanometers to micrometers. The highly porous and reticulate hydrogel structures make BC an ideal skeleton for the fabrication of flexible nanomaterials,[8,9] as various materials are easily coated or functionalized onto BC. In addition, due to its ultrafine structure and pure content, BC exhibits many excellent physicochemical properties such as crystal purity, high tensile strength (200–300 MPa), high porosity,[10] good biocompatibility and excellent flexibility.[11,12] These desirable properties make BC attractive for several fields, especially for flexible electronic devices.[13–15]

However, raw BC exhibits no electrochemical properties. Materials with excellent conductivity are necessary when fabricating BC-based nanoconductive materials.[16,17] Electrically conductive polymers (ECPs), such as polypyrrole (PPy) and polyaniline (PANI), have been widely coated onto BC surfaces to synthesize conductive composites.[13,18] Due to their inherent fast redox switching, high conductivity, low weight and mechanical flexibility, these nonmetal polymers have been widely introduced for loading onto BC surfaces to synthesize ideal conductive composites.[19] PPy has been demonstrated to be well wetted with BC fibers,[20] and PPy/BC nanocomposites have been demonstrated to have potential applications in supercapacitors.[8,21] Nevertheless, the conductivity of BC-based ECPs still needs to be improved, as the porosity of these entirely nonmetal polymers cannot sufficiently support charge transfer.[16,19]

In this regard, several metals have been introduced into BC polymers[17,22] to fabricate more suitable conductive flexible nanocomposites. Tin dioxide (SnO_2) nanoparticles were successfully decorated onto BC films during BC production by cultivation of *Gluconacetobacter xylinum* in Hestrin–Schramn (HS) medium. However, the as-synthesized BC-SnO_2 composites only achieved conductivity properties after pyrolysis at high temperature,[23] which makes the fabrication of these composites more complicated. Antimony tin oxide (ATO), because of excellent conductivity and transparency, is widely used in photoelectric displays, solar cells and transparent electrodes.[24,25] ATO is commonly fabricated by combining SnO_2 and antimony nanoparticles, where Sb replaces Sn during fabrication and notably increases the conductivity.[26] Thus, the introduction of ATO onto BC may directly increase the conductivity of the as-synthesized composites without pyrolysis.

In this study, ATO nanoparticles were first loaded onto BC films during the production of BC, and a transparent conductive film was initially fabricated. Then, the as-prepared BC-ATO films were further coated by the PPy polymers to fabricate PPy-BC-ATO. The structure and electrochemical properties of the as-synthesized conductive materials were also characterized.

EXPERIMENTAL PROCEDURE

Preparation of BC

Bacterial cellulose was synthesized according to a previous study.[27] Briefly, *Acetobacter xylinum* was first cultivated in a preculture medium: glucose (20.0 g/L), peptone (5.0 g/L) and yeast extract (5.0 g/L); initial pH of 6.5 to increase the bacterial population. Then, bacteria were transferred into Hestrin–Schramm (HS) medium and cultivated statically at 30°C for 7 days for BC production. The BC cellulose pellicles were harvested and washed with 0.2 M NaOH at 80°C overnight to remove the residues and then washed with distilled water several times to neutralize the pH.

Synthesis of Composites

The ATO nanoparticle (purchased from Jikangxin Material Company, Hangzhou, China) suspension was prepared by dissolving the nanoparticles in distilled water under ultrasound for 15 min, and γ-(2,3-epoxypropoxy) propytrimethoxysilane (KH-560) was used as the coupling agent. To load as many ATO nanoparticles as possible onto the three-dimensional (3D) structure of the BC, three different fabrication methods were compared: (1) 100 ml prepared 2% ATO suspension was added into the HS medium before cultivation of *Acetobacter xylinum*; (2) 100 ml prepared 2% ATO and 2% KH-560 mixture was added into the HS medium before cultivation for in situ fabrication; (3) 100 ml 2% KH-560 suspension was first added to the HS medium before cultivation, and then 100 ml 2% ATO suspension was added when BC pellicles were grown to approximately 0.5 cm thick. The loading amount of ATO nanoparticles was compared, and the method with the largest loading ratio of ATO nanoparticles (method 2) was selected for the subsequent experiments.

PPy was coated onto the prepared BC-ATO in situ by the oxidative polymerization of pyrrole with $FeCl_3$ as the oxidant and HCl as the dopant. The BC-ATO slices (4 cm × 2 cm) were first mixed with pyrrole and N,N-dimethylformamide (DMF), and then $FeCl_3$ and 37% HCl were slowly added into the mixture. The above prepared mixtures were set at 0°C for 6 h to obtain BC-ATO-PPy. The BC-ATO-PPy was then washed with acetone three times and washed with distilled water three times again to remove impurities. Samples were dried at 60°C for 12 h. BC-PPy was also synthesized by using dried pure BC film by oxidative polymerization as described above. The improved electrochemical properties were compared between BC-PPy and BC-ATO-PPy. A schematic illustration of these composite preparations is shown in Fig. 1.

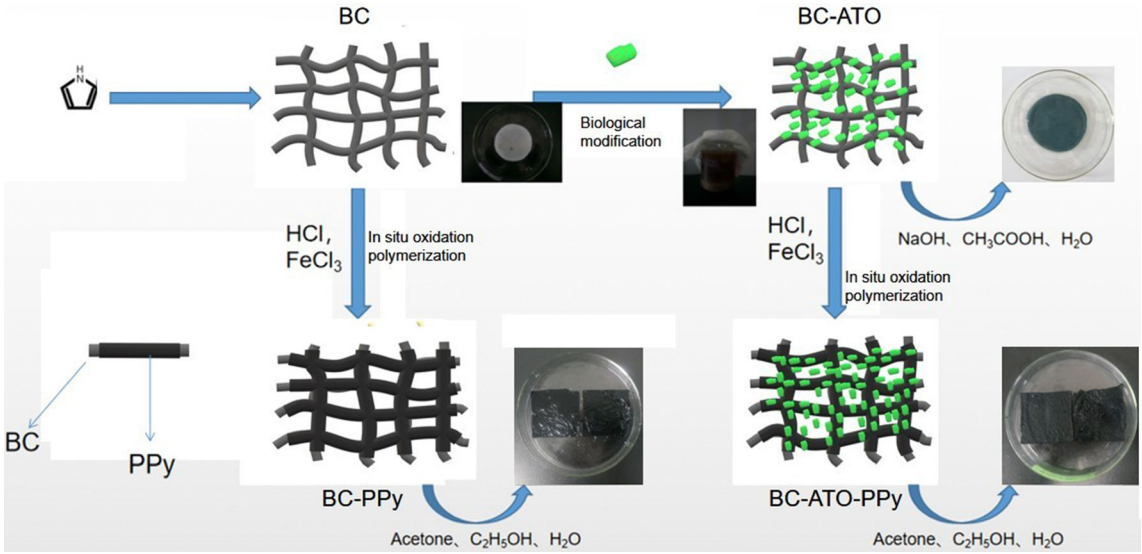

Fig. 1. Schematic illustration of the composite preparation.

Characterization of Composites

Field emission scanning electron microscopy (FE-SEM) was carried out to investigate the structure and morphology of these prepared composites. Briefly, prepared samples were sputtered with gold for 120 s using an ion sputter coater (SC-701 Quick Coater, Japan), and then the in-sections of the samples were observed at 10,000 × to 30,000 × magnification with a field emission scanning electron microscope (JSM-7001F, Jeol, Japan) operated at 10.0 kV. The prepared composites were mixed with spectroscopic-grade potassium bromide powder (1% w/w), and then the functional structure of the samples was investigated by Fourier transform infrared (FT-IR) spectroscopy in a 400–4000 cm^{-1} wavelength range at a 4 cm^{-1} resolution by using an FT-IR spectrometer (Vertex70, Bruker, Germany). The thermal degradation behavior of all prepared composites was determined by a thermogravimetric analyzer (STA 449F3, Netzsch, Germany) between 50°C and 600°C with a heating rate of 10°C/min under a nitrogen atmosphere with a flow rate of 70 ml/min. x-ray diffraction (XRD) was carried out to analyze the phase structure of the composites. Prepared composites were scanned from 5 to 60° (2θ range) at a scan speed of 0.5°/min by using a D/max-RAX x-ray diffractometer (D8 Advance, Bruker, Germany) with Cu Kα radiation (λ=0.154 nm) operated at 40 kV and 30 mA.

Electrochemical Measurements

The electrochemical measurements of these prepared composites were determined by cyclic voltammetry (CV) and electrochemical impedance spectroscopy (EIS). Both tests were carried out using a three-electrode system, including the composite as the working electrode, saturated calomel as the reference electrode and a platinum wire as the counter electrode. The capacitance characteristics of the samples were measured by the CV test using an electrochemical workstation (CHI660C, Shanghai Chenghua, China), and the shape of the CV curve was observed by scanning the samples in a range of different scan rates (10, 20, 30, 50 mV/s). The charge transfer behavior and supercapacitor performance were determined by the Voorburg curve through EIS detection, and the EIS measurements were carried out in a frequency range from 1 Hz to 100 kHz. The electrical conductivity of all as-synthesized composites was measured by a portable four-probe tester (M3, Suzhou Lattice Electronics Co., Ltd., China) at room temperature.

RESULTS AND DISCUSSION

After adding different amounts of KH-560 (0%, 1% and 2%) into the medium, the production of dry BC was similar between these groups (Fig. 2a). This result suggested that adding 2% KH-560 to the medium had no adverse effect on BC production. Figure 2b shows the loading amount of ATO onto the BC by different fabrication methods. Method 2 provided the largest loading amount of ATO (64.50%), followed by method 3 (57.11%) and method 1 (49.62%). This result suggested that the coupling of ATO and KH-56 was beneficial to the in situ loading of ATO onto BC. The lower loading amount of ATO from method 1 may be due to the sinking of ATO during BC production. Thus, method 2 was used to fabricate BC-ATO films in subsequent experiments.

The morphologies and microstructures of the as-prepared materials are shown in Fig. 3. The dimensions of raw BC were approximately 34.5–51.7 nm (Fig. 3a), and the image showed that BC exhibited an aggregated and entangled fiber matrix

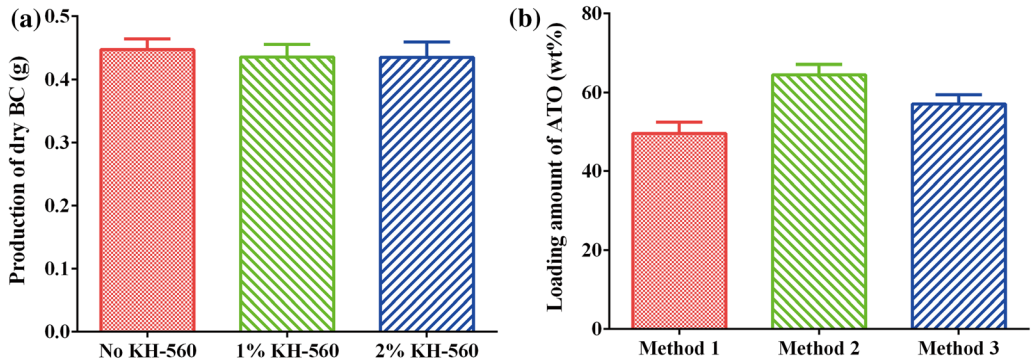

Fig. 2. The effect of KH-560 on BC production (a) and the loading amount of ATO on BC films by different methods (b). Method 1: ATO suspension was added to the HS medium before cultivation; method 2: ATO and KH-560 mixture was added to the HS medium before cultivation; method 3: KH-560 suspension was first added, and ATO was then added after the BC pellicles were grown to approximately 0.5 cm thick.

and presented an interconnected three-dimensional porous network structure, which was in agreement with previous reports.[17,28] Although ATO (Fig. 3c) is composed of tin oxide (SnO2) and antimony, Sb will be present within the SnO_2 lattice.[29] Thus, no Sb nanoparticles were observed under 30000 × magnification by FE-SEM (Fig. 3d). Figure 3e shows that the ATO nanoparticles could be loaded evenly onto the ultrafine structure of the BC. The diameters of BC and ATO in the composites were similar to those of pure materials, and the ATO nanoparticles were largely adhered to BC fibers. Figure 3b shows that raw BC fibers were successfully coated by an irregular PPy, which is similar to previous studies that demonstrated the nonaggregation of PPy during the fabrication of BC-PPy.[16,30] Then, the PPy was also homogeneously coated onto the surface of BC-ATO (Fig. 3f), suggesting the successful fabrication of BC-ATO-PPy.

The structures of the as-prepared materials were investigated by FT-IR and XRD. The FT-IR results are shown in Fig. 4. The characteristic peaks of raw BC, PPy and ATO were all detected by FT-IR (Table I). Compared to BC, the characteristic peaks (3448 cm^{-1}, 2925 cm^{-1}, 1078 cm^{-1}, 617 cm^{-1}) of ATO were observed for the BC-ATO composites (Table I), which demonstrated the successful fabrication of BC-ATO composites. Furthermore, extra characteristic peaks of PPy (1477 cm^{-1}, 1314 cm^{-1}, 1176 cm^{-1}, 918 cm^{-1}) were observed for the BC-ATO-PPy composites, revealing the successful fabrication of BC-ATO-PPy. Thus, the characteristic peaks of the synthesized materials may well demonstrate that ATO and PPy can be coated onto the surface of BC films.

XRD patterns of the as-prepared materials are shown in Fig. 5. Raw BC samples (line A) exhibited diffraction peaks at 2Θ angles of 14.25°, 16.56° and 22.55°, which correspond to the ($1\bar{1}0$), (110) and (200) crystal planes, respectively, and indicate cellulose I. Compared to pure BC films, BC-ATO displayed several other diffraction peaks (26.85°, 34.09°, 38.29°, 52.04°, 54.98°, 57.03°), which may be attributed to SnO_2. However, no diffraction peaks of antimony oxide were observed, suggesting the dispersion of antimony in ATO nanoparticles.[31] PPy displayed diffraction peaks of 16°, 27°, 42° and 53° (shown in line C). Thus, all the diffraction peaks of BC, ATO and PPy were observed in the as-synthesized BC-ATO-PPy composite (line B), suggesting the successful fabrication of this composite. According to a previous report,[32] the crystallinity index (CI) of various materials was calculated as 97.3% BC, 76.0% PPy, 93.6% BC-ATO and 89.6% BC-ATO-PPy.

The thermal stabilities of these materials were compared by TGA curves (Fig. 6). Compared to pure BC films (line A), the thermal stability of all as-synthesized nanocomposites was obviously increased. The increase in thermal stability of the nanocomposites can be attributed to the higher decomposition temperature of PPy and the non-decomposition of ATO at high temperature. In a previous study, the degradation of PPy occurred at 460° C, which greatly improved the thermal stability of the composite materials.[33] In another report, the incorporation of ATO nanoparticles within the polymers improved the thermal stability of the resulting nanocomposite membranes, which is similar to the present results.[34] The initial decomposition of the BC was 195°C, while it was increased to approximately 266°C for the as-synthesized composites. The first decomposition stage was 266°C to 400°C for the as-synthesized composites, which could be attributed to the pyrolysis of the BC and was similar to pure BC. For BC-ATO, the final weight loss was approximately 29.6%, which may be due to the pyrolysis of the BC. Compared to pure BC, the BC-ATO composite had higher thermal stability resulting from the coating of ATO nanoparticles. A weight loss of approximately 49.4% for BC-PPy was observed at 722°C, including a 12.1% weight loss due to the pyrolysis of PPy from 396°C to 722°C. The thermal stability was significantly increased compared to pure BC, which may be attributed to the carboxylate moieties created by

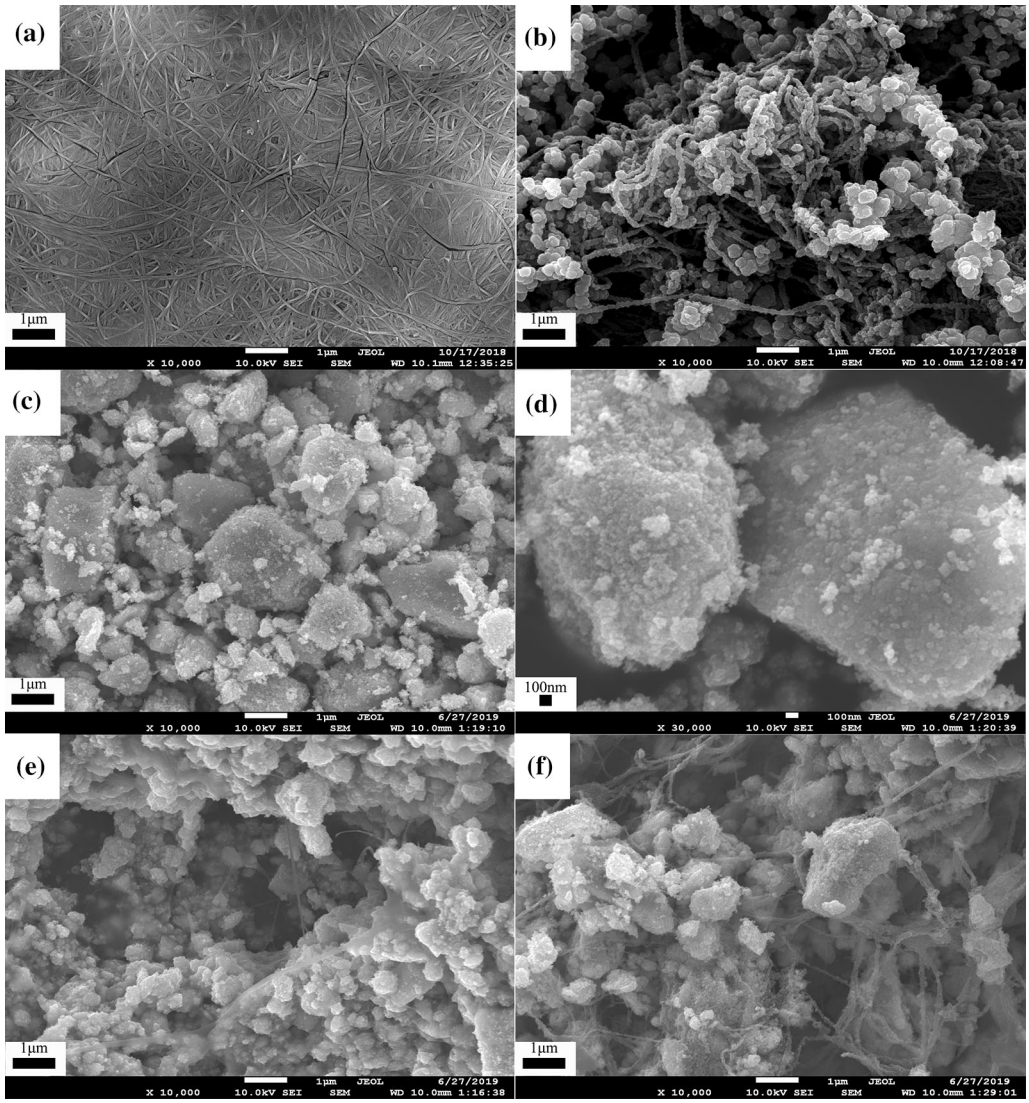

Fig. 3. FE-SEM images of the as-synthesized materials. BC (a), BC-PPy (b), SnO_2 under 10,000× magnification (c), SnO_2 under 30,000× magnification (d), BC-ATO (E), BC-ATO-PPy (f).

Table I. The characteristic peaks of pure materials (BC, PPy, ATO)

Material	Characteristic peaks (cm^{-1})							
BC	2910	1637	1066	898				
PPy	1552	1477	1314	1176	918			
ATO	3448	2925	1423	1034	617			
BC-ATO*	3448	2925	1078	617				
BC-ATO-PPy*	3448	2925	1078	617	1477	1314	1176	918

*The extra peaks were detected in the composites, but were not detected in the pure BC film

the connection of BC and PPy.[16] The final weight loss of BC-ATO-PPy was approximately 65.3% at 720°C, and 13.0% resulted from the pyrolysis of PPy from 402°C to 720°C. Thermogravimetry[23] calculations show that the weight percentage of ATO was 59 wt.% in BC-ATO and 26.7 wt.% in BC-ATO-PPy, which was consistent with the final resting weight of these as-synthesized composites and further demonstrated the successful fabrication of the nanocomposites.

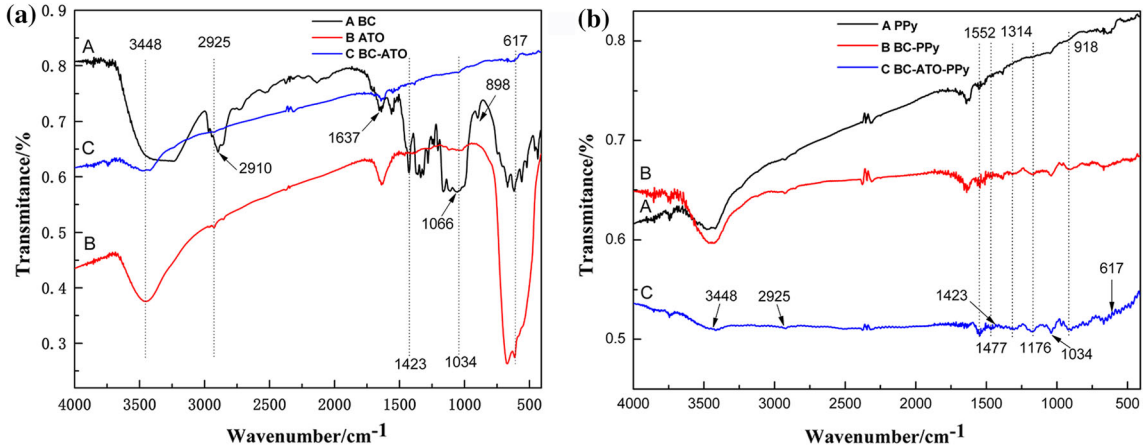

Fig. 4. Infrared spectra analysis of prepared materials. The infrared spectra of BC, ATO and BC-ATO (a). The infrared spectra of PPy, BC-PPy and BC-ATO-PPy (b).

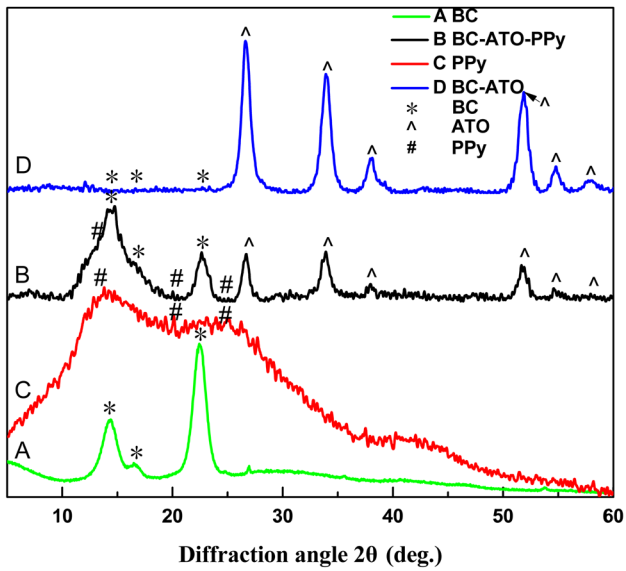

Fig. 5. XRD diffraction peaks of the as-prepared materials.

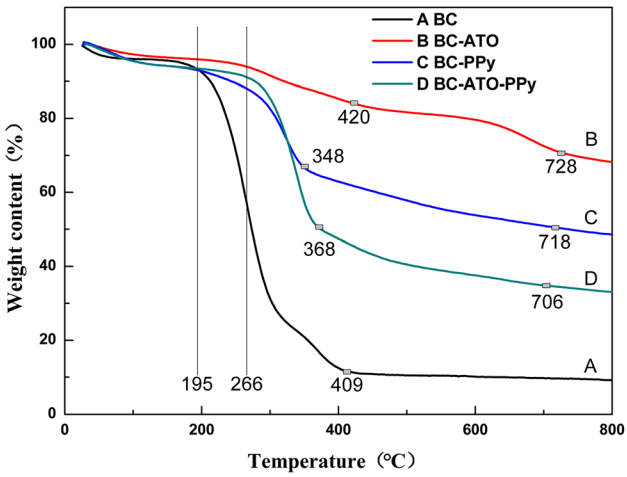

Fig. 6. TGA curve of the as-prepared materials.

The capacitance characteristics of BC and other as-synthesized composites were evaluated using cyclic voltammetry (CV) tests. No oxidation peaks or reductions were observed for pure BC films at different scanning speeds (Fig. 7a), which had been demonstrated in previous studies.[16,33] The characteristic redox behavior was only observed in the as-synthesized BC-ATO nanocomposites (Fig. 7b). Similar results were obtained in previous studies, in which redox behavior was observed for the BC-SnO_2 composite but not for BC-SnO_2-PPy or BC-PPy.[35] SnO_2 and ATO exhibited asymmetric redox peaks, as demonstrated in a previous study.[29] However, when the PPy coated uniformly outside the films or composites, the redox behavior may disappear for BC-ATO-PPy (Fig. 7d). Although no redox behavior was observed in BC-PPy (Fig. 7c) and BC-ATO-PPy, the CV shapes were well retained as the scan rate increased from 10 mV/s to 50 mV/s. This result suggested that these composites had good capacitance characteristics and charge–discharge rates. A bending test was carried out to investigate the flexible and recoverable conductivity properties of BC-ATO-PPy. No obvious changes in CV curves were observed at different bending deformations (Fig. 7e), suggesting negligible changes in capacitance characteristics under various bending tests. The specific capacitance was increased from 7.47 F/g for BC to 681.3 F/g for BC-ATO-PPy, 563.9 F/g for BC-ATO and 302.2 F/g for BC-PPy (Table II). The capacitance retention of all materials was kept stable after 100 charge–discharge cycles (Fig. 7f). These results revealed that BC supplied the necessary flexible and recoverable properties in these as-synthesized BC-based nanocomposites, while the ATO and PPy fabricated onto the BC helped to increase the electrochemical performance.

A four-probe test showed that BC-ATO-PPy had the highest conductivity (16.532 S/cm), followed by BC-PPy (11.636 S/cm) and BC-ATO (10.236 S/cm) (Table II). These results indicated that both ATO and PPy contributed to increasing the conductivity

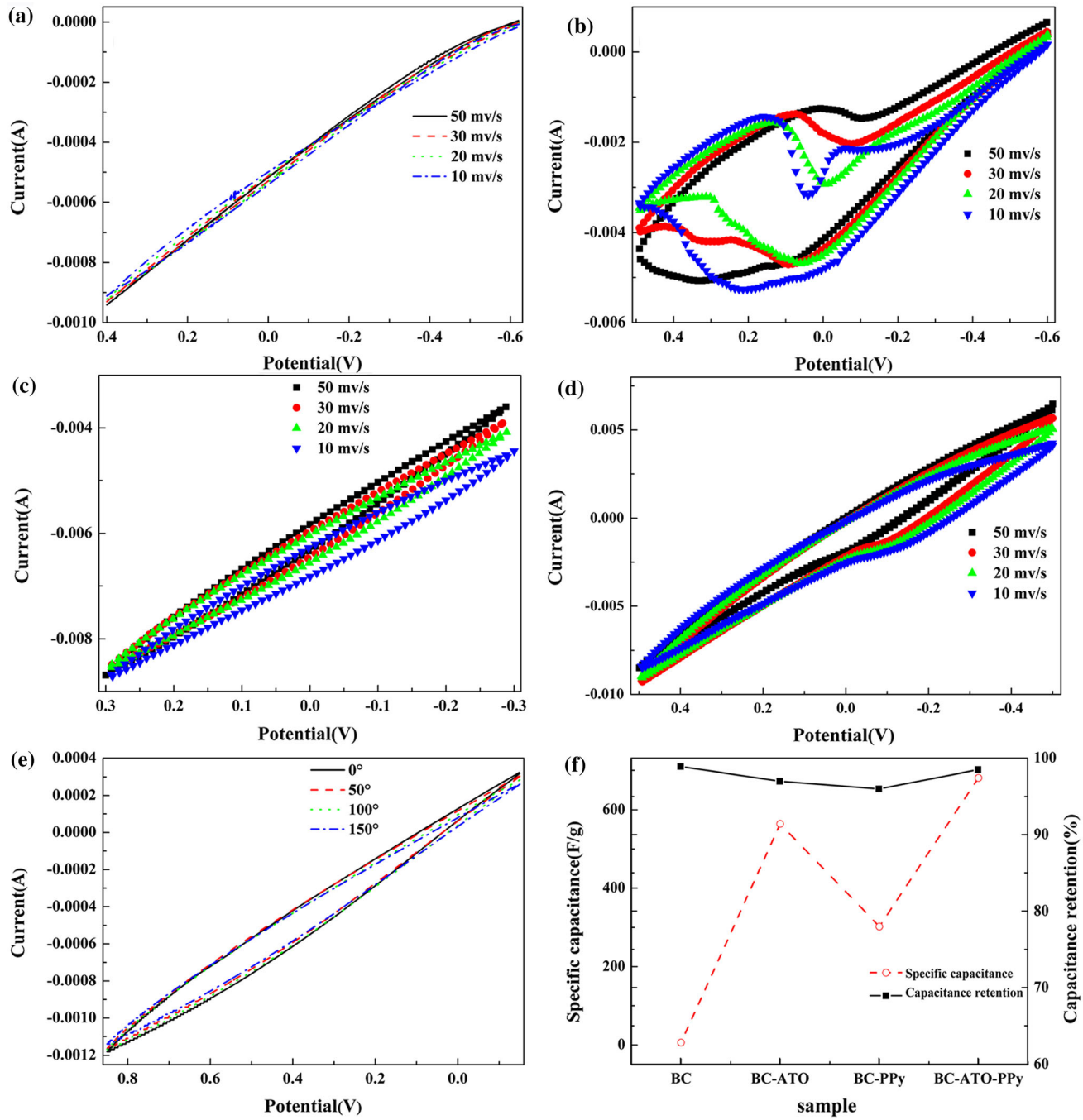

Fig. 7. The electrochemical characterization of the as-prepared materials. Cyclic voltammograms at various scan rates: BC (a), BC-ATO (b), BC-PPy (c), BC-ATO-PPy (d) and BC-ATO-PPy (e) at different bending tests. Specific capacitance and capacitance retention of each sample (f).

of the as-synthesized BC-ATO-PPy nanocomposites. Similar conductivity for these materials was observed during the bending test (Fig. 8a, Bσ), suggesting that BC-based nanocomposites could serve as excellent flexible conductivity materials. Electrochemical impedance spectroscopy (EIS) was further carried out to evaluate the electrochemical characteristics of these composites. The Warburg curve of these materials is shown in a Nyquist plot (Fig. 8b). The resistance values of these materials were obtained from the intercept of the cure on the X-axis. The lowest resistance value was observed for BC-ATO-PPy (32.4 Ω), followed by BC-PPy (63.2 Ω), BC-ATO (83.6 Ω) and BC (681.5 Ω) (Table II), which was in accordance with the conductivity value obtained by the four-probe test. The lowest resistance value and highest conductivity of BC-ATO-PPy revealed that the as-synthesized BC-ATO-PPy could

Table II. The electrochemical properties of the materials (BC, BC-ATO, BC-PPy, BC-ATO-PPy)

Electrochemical properties	BC	BC-ATO	BC-PPy	BC-ATO-PPy
Resistance/Ω	681.5	83.6	63.2	32.4
Specific capacitance (F/g)	7.47	563.9	302.2	681.3
Conductivity (S/cm)	ND	10.236	11.636	16.532

ND: not detected

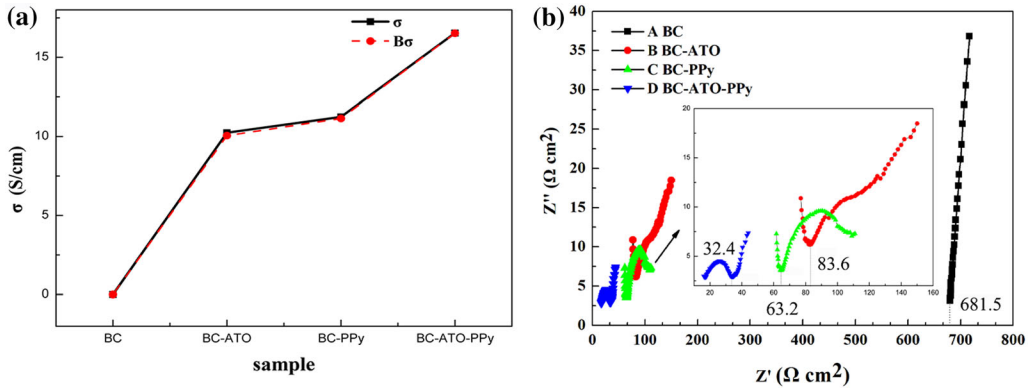

Fig. 8. The resistance value of samples (a) and the EIS curves (b).

be used as a highly conductive material. Both PPy and ATO contributed to the increasing conductivity of BC-based composites. PPy loaded onto the BC ultrafine structure created a continuous conduction pathway on these nanocomposites and increased the conductivity considerably.[8] As an excellent conductive material,[36,37] ATO fabricated onto BC-based composites significantly increased the electrochemical properties of the as-synthesized composites. Thus, the excellent electrochemical performance coupled with the flexible properties of BC films makes BC-ATO-PPy composites highly attractive for electronic device applications.

CONCLUSIONS

In the present study, a bacterial cellulose-based ATO-PPy nanocomposite was synthesized, and its structures were characterized. An electrochemical characterization demonstrated that BC-ATO-PPy is an excellent flexible conductive material. As bacterial cellulose is sustainable, biodegradable and easily obtained, this study offers a promising way to synthesize low-cost and environmentally friendly flexible conductive materials.

ACKNOWLEDGMENTS

The work was partly supported by the National Natural Science Foundation of China (Grant No. 41807401) and the Doctor Support Grants of Zhengzhou University of Light Industry (BSJJ2014066).

CONFLICT OF INTEREST

The authors declare that they have no conflicts of interest.

REFERENCES

1. Y. Chen, F. Wang, L. Dong, Z. Li, L. Chen, X. He, J. Gong, J. Zhang, and Q. Li, *Polymers (Basel)* 11, 96 (2019).
2. L. Ma, R. Liu, H. Niu, L. Xing, L. Liu, Y. Huang, and A.C.S. Appl, *Mater. Interfaces.* 8, 33608 (2016).
3. D. Langley, G. Giusti, C. Mayousse, C. Celle, D. Bellet, and J.P. Simonato, *Nanotechnology* 24, 452001 (2013).
4. Q. Rong, W. Lei, and M. Liu, *Chemistry* 24, 16930 (2018).
5. T. Zhang, L. Yang, X. Yan, and X. Ding, *Small* 14, e1802444 (2018).
6. M.M. Pérez-Madrigal, M.G. Edo, and C. Alemán, *Green Chem.* 18, 5930 (2016).
7. Z. Li, L. Wang, J. Hua, S. Jia, J. Zhang, and H. Liu, *Carbohyd. Polym.* 120, 115 (2015).
8. J. Xu, L.G. Zhu, Z.K. Bai, G.J. Liang, L. Liu, D. Fang, and W.L. Xu, *Org. Electron.* 14, 3331 (2013).
9. L. Zuo, W. Fan, Y. Zhang, Y. Huang, W. Gao, and T. Liu, *Nanoscale* 9, 4445 (2017).
10. I. Reiniati, A.N. Hrymak, and A. Margaritis, *Crit. Rev. Biol.* 37, 510 (2017).
11. W. Hu, S. Chen, Z. Yang, L. Liu, and H. Wang, *J. Phys. Chem. B.* 115, 8453 (2011).
12. V. Thiruvengadam and S. Vitta, *Cellulose* 24, 3341 (2017).
13. A.R. Rebelo, C. Liu, K.H. Schafer, M. Saumer, G. Yang, and Y. Liu, *Langmuir* 35, 10354 (2019).
14. N. Shah, M. Ul-Islam, W.A. Khattak, and J.K. Park, *Carbohyd. Polym.* 98, 1585 (2013).
15. B. Wang, X.L. Li, B. Luo, J.X. Yang, X.J. Wang, Q. Song, S. Y. Chen, and L.J. Zhi, *Small* 9, 2399 (2013).
16. F. Wang, H.J. Kim, S. Park, C.D. Kee, S.J. Kim, and I.K. Oh, *Compos. Sci. Technol.* 128, 33 (2016).
17. M. Ul-Islam, S. Khan, M.W. Ullah, and J.K. Park, *Biotechnol. J.* 10, 1847 (2015).

18. S. Peng, L. Fan, C. Wei, X. Liu, H. Zhang, W. Xu, and J. Xu, *Carbohyd. Polym.* 157, 344 (2017).
19. G. Nystrom, A. Razaq, M. Stromme, L. Nyholm, and A. Mihranyan, *Nano Lett.* 9, 3635 (2009).
20. James H. Johnston, Fern M. Kelly, John Moraes, Thomas Borrmann, and David Flynn, *Curr. Appl. Phys.* 6, 587 (2006).
21. L. Tang, J. Han, Z. Jiang, S. Chen, and H. Wang, *Carbohyd. Polym.* 117, 230 (2015).
22. Y. Yuan, J. Zhou, M.I. Rafiq, S.M. Dai, J. Tang, and W.H. Tang, *Electrochim. Acta* 295, 82 (2019).
23. B. Dursun, T. Sar, A. Ata, M. Morcrette, M.Y. Akbas, and R. Demir-Cakan, *Cellulose* 23, 2597 (2016).
24. J. Lee, N.H. Kim, and Y.S. Park, *J. Nanosci. Nanotechnol.* 16, 4973 (2016).
25. Y. Bai, Y. Fang, Y. Deng, Q. Wang, J. Zhao, X. Zheng, Y. Zhang, and J. Huang, *Chemsuschem* 9, 2686 (2016).
26. L. Liu, T. Kawaharamura, G.T. Dang, E.K.C. Pradeep, S. Sato, T. Uchida, S. Fujita, T. Hiramatsu, H. Kobayashi, and H. Orita, *Jpn. J. Appl. Phys.* 58, 2 (2019).
27. J. Ye, S. Zheng, Z. Zhang, F. Yang, K. Ma, Y. Feng, J. Zheng, D. Mao, and X. Yang, *Bioresource Technol.* 274, 518 (2019).
28. J. Kim, S.W. Kim, S. Park, K.T. Lim, H. Seonwoo, Y. Kim, B. H. Hong, Y.H. Choung, and J.H. Chung, *Adv. Healthc. Mater.* 2, 1525 (2013).
29. Y. Lv, C. Yang, H. Wang, J. Zhang, and Y. Xiang, S, Lu. *Cata. Sci. Technol.* 10, 2484 (2020).
30. S. Peng, Q. Xu, L.L. Fan, C.Z. Wei, H.F. Bao, W.L. Xu, and J. Xu, *Synthetic Met.* 222, 285 (2016).
31. R. Noonuruk, N. Vittayakorn, W. Mekprasart, J. Sritharathikhun, and W. Pecharapa, *J. Nanosci. Nanotechnol.* 15, 2564 (2015).
32. E. Tsouko, C. Kourmentza, D. Ladakis, N. Kopsahelis, I. Mandala, S. Papanikolaou, F. Paloukis, V. Alves, and A. Koutinas, *Int. J. Mol. Sci.* 16, 14832 (2015).
33. X.X. Zhang, M.Y. Gao, L. Tong, and K.F. Cai, *J. Mater.* 6, 339 (2020).
34. B. Khorshidia, S.A. Hosseinia, G. Ma, M. McGregor, and M. Sadrzadeh, *Polymer* 163, 48 (2019).
35. J.B. Ye, L.X. Guo, S.S. Zheng, Y.J. Feng, T.T. Zhang, Z.C. Yang, Q.S. Yuan, G.P. Shen, and Z. Zhang, *Mater. Lett.* 253, 372 (2019).
36. T. Zinchenko, E. Pecherskaya, and D. Artamonov, Aims. *Mater. Sci.* 6, 276 (2019).
37. R. Ostermann, R. Zieba, M. Rudolph, D. Schlettwein, and B. M. Smarsly, *Chem. Commun.* 47, 12119 (2011).